

## Article

# Characteristics and Geological Significance of Organic Matter Veins in Shale Reservoir: A Case Study of the Silurian Longmaxi Formation in Luzhou Area, Sichuan Basin

Yuanlin Wang<sup>1,2</sup>, Yunqian Jia<sup>1,2</sup> , Chenchen Wang<sup>2,3,\*</sup> , Wei Lin<sup>4</sup> , Jizhen Zhang<sup>2,5</sup>, Denglin Han<sup>1,2</sup>, Binyu Ma<sup>1,2</sup> and Huachao Wang<sup>6</sup>

- <sup>1</sup> School of Geosciences, Yangtze University, Wuhan 430100, China; wangyl.st@yangtzeu.edu.cn (Y.W.); jiajq@yangtzeu.edu.cn (Y.J.); handl@yangtzeu.edu.cn (D.H.); mabinyu2011@163.com (B.M.)
- <sup>2</sup> Laboratory of Reservoir Microstructure Evolution and Digital Characterization, Yangtze University, Wuhan 430100, China; zhangjz1991@126.com
- <sup>3</sup> Cooperative Innovation Center of Unconventional Oil and Gas, Yangtze University, Wuhan 430100, China
- <sup>4</sup> Institute of Geology and Paleontology, Linyi University, Linyi 276000, China; ucaslinwei@126.com
- <sup>5</sup> College of Resources and Environment, Yangtze University, Wuhan 430100, China
- <sup>6</sup> No. 3 Oil Production Plant, PetroChina Changqing Oilfield Company, Yinchuan 750006, China; 201671258@yangtzeu.edu.cn
- \* Correspondence: wcc1220@163.com

**Abstract:** Organic matter serves as the hydrocarbon-generating parent material for shale reservoirs, in which organic pores are also important reservoir spaces. Different types of organic matter have wide differences in hydrocarbon generation and pore-forming ability. Based on the occurrence state of organic matter, in the over-mature Marine shale organic matter mainly includes in situ and migrated organic matter. It has been extensively studied on in situ organic matter and organic matter migrating into inorganic pores, while there are few reports of organic matter migrating into microfractures. In this study, the over-mature Marine shale reservoir in the first sub-member of the Silurian Longmaxi Formation in the Luzhou area of the Sichuan Basin is taken as an example. Core observation, optical microscope, high-precision large-view scanning (MAPS, modular automated processing system) and mineral analysis scanning (QEMSCAN, quantitative evaluation of minerals by scanning electron microscopy) were conducted to observe the morphological characteristics of organic matter veins, and then analyze the genesis and pore-forming characteristics of such organic matter. The results show that: ① Organic matter veins (OM veins) are soluble organic matter with fractures as an effective channel, and OM veins in the study section is easy to form under the condition of microfractures in the shale sweet segment after organic matter generating oil and before gas generation ② Organic matter in the OM veins are less efficient in pore-forming, with sparse pores and smaller pore sizes. The occurrence of fractures varies greatly, including horizontal fractures, oblique fractures and high-angle fractures, which are mostly developed in the Long1<sub>1</sub><sup>1</sup> and Long1<sub>1</sub><sup>2</sup> layers. ③ The development of OM veins can indicate better reservoir conditions, that is, the layers have strong hydrocarbon generation intensity (strong pore-forming ability of organic matter) and high brittle mineral content (strong reservoir compressibility). The new findings in this paper reveal that OM veins are instructive for the determination of geological–engineering sweet spots in the Longmaxi Formation in the Sichuan Basin, and also provide guidance for future research on occurrence form and geological significance of different types of organic matter.

**Keywords:** Sichuan Basin; Luzhou area; Longmaxi Formation; scanning electron microscope; organic matter type



**Citation:** Wang, Y.; Jia, Y.; Wang, C.; Lin, W.; Zhang, J.; Han, D.; Ma, B.; Wang, H. Characteristics and Geological Significance of Organic Matter Veins in Shale Reservoir: A Case Study of the Silurian Longmaxi Formation in Luzhou Area, Sichuan Basin. *Minerals* **2023**, *13*, 1080. <https://doi.org/10.3390/min13081080>

Academic Editors: Ruyue Wang, Mengdi Sun, Shang Xu, Songtao Wu, Jianhua Zhao, Yiquan Ma, Jianhua He and Thomas Gentzis

Received: 29 June 2023

Revised: 4 August 2023

Accepted: 10 August 2023

Published: 14 August 2023



**Copyright:** © 2023 by the authors. Licensee MDPI, Basel, Switzerland. This article is an open access article distributed under the terms and conditions of the Creative Commons Attribution (CC BY) license (<https://creativecommons.org/licenses/by/4.0/>).

## 1. Introduction

Organic matter is the parent material of hydrocarbon generation, and organic pores serve as significant reservoir spaces [1,2]. Therefore, the pore-forming ability of organic

matter is a key parameter in evaluation of unconventional petroleum systems [3,4]. Previous studies have shown that different types of organic matter have great differences in hydrocarbon generation and pore-forming capacity [5–7]. At present, the classification methods of over-mature Marine organic matter types are mostly based on morphology from the perspective of organic matter sources, and it is widely believed that bitumen and kerogen are the main components of organic matter [8]. Loucks et al. determined seven petrological criteria based on the occurrence of organic matter in SEM micrographs, which can be used to distinguish sedimentary organic matter from migrating organic matter according to the occurrence pore, the continuous distribution, dense texture of organic matter and so on [9]. On this basis the migrating organic matter was further divided into morphological and amorphous forms, and algal fragments, bacterial aggregates, graptolites and microsomes were identified from kerogen [10,11]. The hydrocarbon generation capacity and pore evolution process of different organic matter types are also different, the organic matter filled in the intergranular pores of rigid mineral particles has a high degree of development, which is the best for the development of organic matter macropores, and in the mixture of organic matter and clay minerals, the pore size distribution range is wide but the total amount of organic pores is small [12–14].

In conclusion, many studies have shown that a large amount of migrated organic matter in the pores of inorganic minerals exists in the over-mature Marine shale reservoir of Longmaxi Formation, Sichuan Basin, which plays an important role in the formation of shale gas [15]. In contrast to that the organic matter migrated to microfractures is rarely reported. It is worth noting that the organic matter migrating to the fracture is different from the shrinkage fracture of organic matter developed at the edge of the banded organic matter mentioned in previous studies [16]. Although all of them are in the form of organic matter in the fracture, the organic matter referred to by the predecessors is a long strip of in-situ organic matter. The most obvious feature is that the outline is clear and does not interact with clay minerals. In this study, the organic matter which was migrated and filled into microfractures, was called organic matter veins (OM veins). shale fractures and their corresponding filled veins are important features for restore the process of hydrocarbon generation with important implications for studying shale gas enrichment and preservation [17]. The characteristics of temperature, pressure and diagenetic fluid environment recorded by calcite, quartz and other minerals in fracture veins have been extensively reported [18,19]. Therefore, this study combines organic matter type, veins and fracture open-closure times to explore the indicative significance of OM veins to shale reservoir.

In this manuscript, we characterize OM veins at multiple scales and parameters, and analyses the morphological characteristics, occurrence state and pore-forming ability of organic matter in fractures based on core observation, optical microscope, MAPS high-resolution large-field scanning and QEMSCAN mineral analysis scanning under the same field of view. The research also discusses the distribution, source and formation period of OM veins, and then to explore the geological significance of OM veins. in order to systematically understand the formation and evolution of different organic matter in shale reservoirs, and provide more detailed microscopic evaluation for shale gas desserts.

## 2. Geological Setting

The study area is mainly the Luzhou area in the southern Sichuan Basin, which is structurally located in the low-steep structural belt in southern Sichuan. From north to south, the comb-shaped anticline structure arranged in an echelon is developed. The syncline structure is wide and gentle, and small-scale faults are mainly developed, which have little damage to shale gas reservoirs [20,21]. In terms of sedimentation, since the early Cambrian, the basin has generally been in a shallow sea environment. Due to the influence of rising ocean currents, the area has formed a paleogeographic environment conducive to the deposition of shale and phosphorus [22].

From Ordovician to Early Silurian, the Sichuan Basin was surrounded by the Chuanzhong uplift, the Xuefeng uplift, and the Qianzhong uplift [23]. The Sichuan Basin was surrounded by the east, west, and south sides, forming a restricted retention basin environment favorable for the development of source rocks, resulting in the terrain of “three uplifts and one depression” [24,25] (Figure 1). At the end of Ordovician and the beginning of Silurian, two global transgressions [26,27] and multi-stage large-scale volcanic activities occurred [28], forming the shale of the Wufeng–Longmaxi formation. Since the early deposition of the Longmaxi formation, the Luzhou area as a whole was located in the deep-water shelf sedimentary environment [29] and was in a quiet anoxic environment [30].

The first member of the Longmaxi formation is divided into Long1<sub>1</sub> and Long1<sub>2</sub> sub-members. Long1<sub>1</sub> sub-member is mainly organic-rich shale, and the TOC value is generally higher than 2.0%. According to the lithology, stratigraphic sequence, sedimentary cycle and paleontology of typical wells, Long1<sub>1</sub> sub-member is subdivided into Long1<sub>1</sub><sup>1</sup>, Long1<sub>1</sub><sup>2</sup>, Long1<sub>1</sub><sup>3</sup> and Long1<sub>1</sub><sup>4</sup> layers from bottom to top [31].

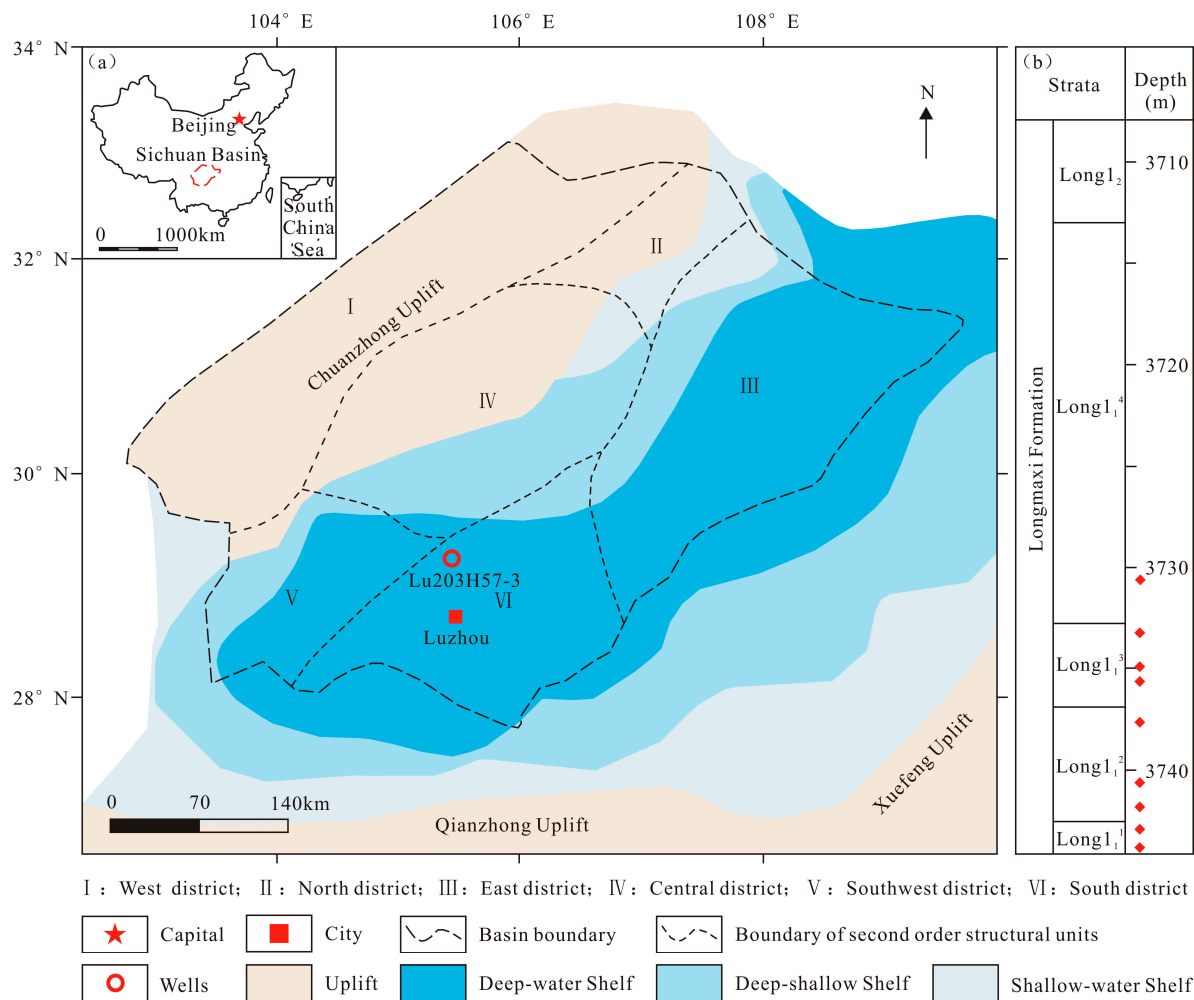


**Figure 1.** (a) Regional geological map of Sichuan Basin (modified after [32–35]). (b) Stratigraphic column.

### 3. Samples and Methods

#### 3.1. Research Samples

A total of 9 representative samples from Silurian Long1<sub>1</sub> sub-member of Well Lu 203H57-3 in the Luzhou area were included in this study. The samples covered thin layers of Long1<sub>1</sub><sup>1</sup>–Long1<sub>1</sub><sup>4</sup> with a depth of 3720~3750 m. After sampling, the fresh samples were

packaged and immediately sent to the Laboratory of Reservoir Microstructure Evolution and Digital Characterization of Yangtze University for sample preparation and experiment.

### 3.2. Experimental Method

In view of the extremely fine-grained sedimentary fabric characteristics and strong heterogeneity of shale, the MAPS scanning technology with high resolution (500 nm) and large field of view (the physical size of the sample is centimeter level) is used to scan the sample as a whole. Scanning technology is used to divide the sample surface area into a series of regular grids, and then scan and create an image of each grid to obtain a series of two-dimensional high-resolution scanning images. Then, all images are spliced to obtain a complete two-dimensional high-resolution large-field scanning image [36]. The test method is based on SY/T 5162-2014.

In view of the fact that the pores of organic matter in shale are at the nanoscale, organic matter in different occurrence states is located and statistically analyzed from the complete MAPS images, and a single image with a higher resolution (4 nm) is obtained. A total of 140 images are captured, including 20 of in situ organic matter, 40 of organic matter in inorganic pores and 80 of OM veins. Using the image-segmentation technology of ImageJ software, the pores in organic matter were extracted from single images of different organic matter types [37], and the pore-forming efficiency was calculated [7]. Porosity measuring standards observe SY/T6103-2019. Specifically, porosity parameters of different samples were collected and the mean of multiple operations by different people was used. On this basis, the statistical errors caused by image factors and artificial factors can be avoided to the maximum extent.

In order to accurately obtain the mineral distribution and content information under MAPS scanning images, QEMSCAN mineral analysis scanning technology was used to scan the same field of view. The scanning technology is based on the energy of X-ray generated by the primary electron in the process of atomic excitation of secondary electrons on the surface of the sample to determine the element type of the object in the scanned point. According to the element distribution information, the actual elements are combined into minerals in the background mineral species database, and then the mineral distribution and content information are obtained. The test method is based on GB/T 17359-2012 and GB/T 20726-2015. The test result is a two-dimensional color image. Different color areas represent different mineral components, and white areas represent non-mineral components such as pores, cracks, and organic matter. Corresponding to the MAPS image in the same field of view, the white area components can be accurately identified.

The instrument used for MAPS scanning is HELIOS NanoLab 650, the voltage is 1~30 KV, the current is 0.78 pA~26 nA, the pixel size of the recognition image is 2~800 nm, and the overlap rate between adjacent spliced small images is 6~8%. The QEMSCAN scanning instrument is QEMSCAN 650F, the voltage is 1~30 KV, the current is 0.78 pA~26 nA, and the pixel size of the recognition image is 0.5~50  $\mu\text{m}$ . The laboratory temperature is  $20 \pm 5$  °C, and the humidity is not more than 60%.

In addition, in order to fully obtain the characteristics of shale reservoirs, LECO carbon and sulfur analyzer CS230 was used to determine the total organic carbon (TOC) content of the samples, and the test method was based on GB/T 19145-2022.

## 4. Results

### 4.1. Morphological Characteristics

According to the source of organic matter and its occurrence under SEM, the types of organic matter in the study section are divided into in situ sedimentary organic matter, organic matter migrating to inorganic pores and organic matter migrating to fractures (OM veins). Among them, the in situ organic matter is the most primitive organic matter deposited in the process of sedimentation, so it retains some biological structure characteristics. However, because it comes from different organic components, its morphological performance is not exactly the same (Figure 2a,b). But as a whole, the area of in situ organic

matter is large and the boundary between the organic matter and mineral particles is also obvious. The organic matter in the inorganic pores is the most common type of organic matter in the studied section [5], and it is the bitumen generated by in situ organic matter in the process of hydrocarbon generation and expulsion. The area of organic matter in inorganic pores is small and its morphology is controlled by the pores of the mineral matrix before filling, which include intergranular pores, pyrite intercrystalline pores, clay mineral interlayers, and mineral particle cracks (Figure 2c,d). The organic matter in the fracture usually runs through the entire scanning electron microscope field of view with an opening of 5~80  $\mu\text{m}$  (Figure 3).

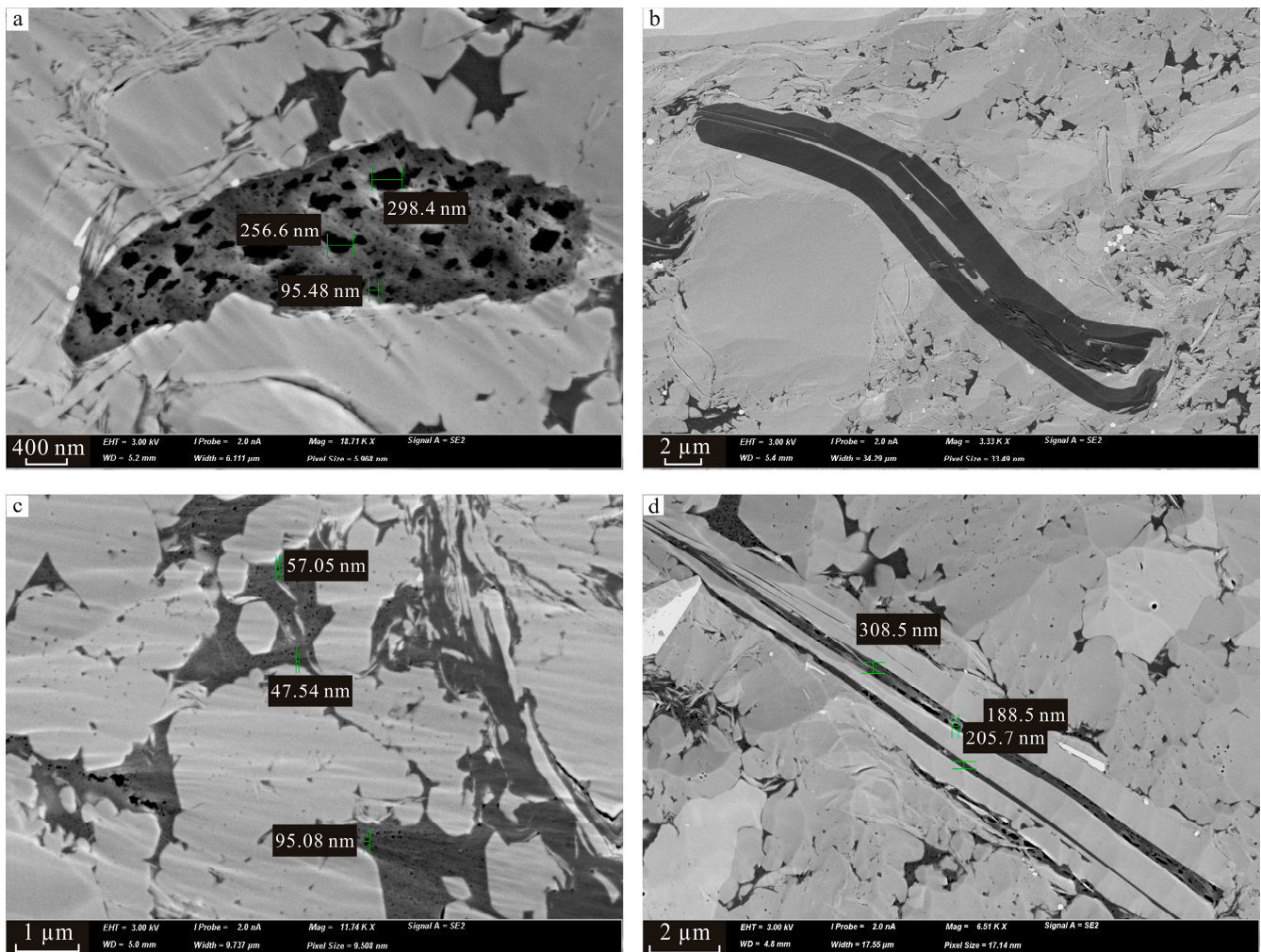


**Figure 2.** Scanning electron microscope image of Long<sub>1</sub> sub-member of Lu203H57-3 well. (a) In situ organic matter of spropelinite, in which the pores are alternate in size and dense (Long<sub>1</sub><sup>3</sup> layer, 3733.2 m). Spropelinite has neither fixed morphology nor clear contour. It is mainly flocculent or cloudiness and can adapt its morphology continuously to matrix pores. (b) In situ organic matter of inertinite, low degree of pore development (Long<sub>1</sub><sup>3</sup> layer, 3734.9 m). The longitudinal section of inertinite fusinite is fibrous and fusinite is in bedding arrangement. (c) Intergranular organic matter, small and dense pores (Long<sub>1</sub><sup>1</sup> layer, 3743.8 m). (d) Organic matter inside clay minerals, small and dense pores (Long<sub>1</sub><sup>2</sup> layer, 3741.8 m).

OM veins can also be observed in core hand specimens and optical microscope, they obliquely cross bedding and are black and irregular (Figure 4). Ordinary slices show that organic matter is mostly filled into horizontal fractures and clay minerals such as illite are often found around them (Figure 5).

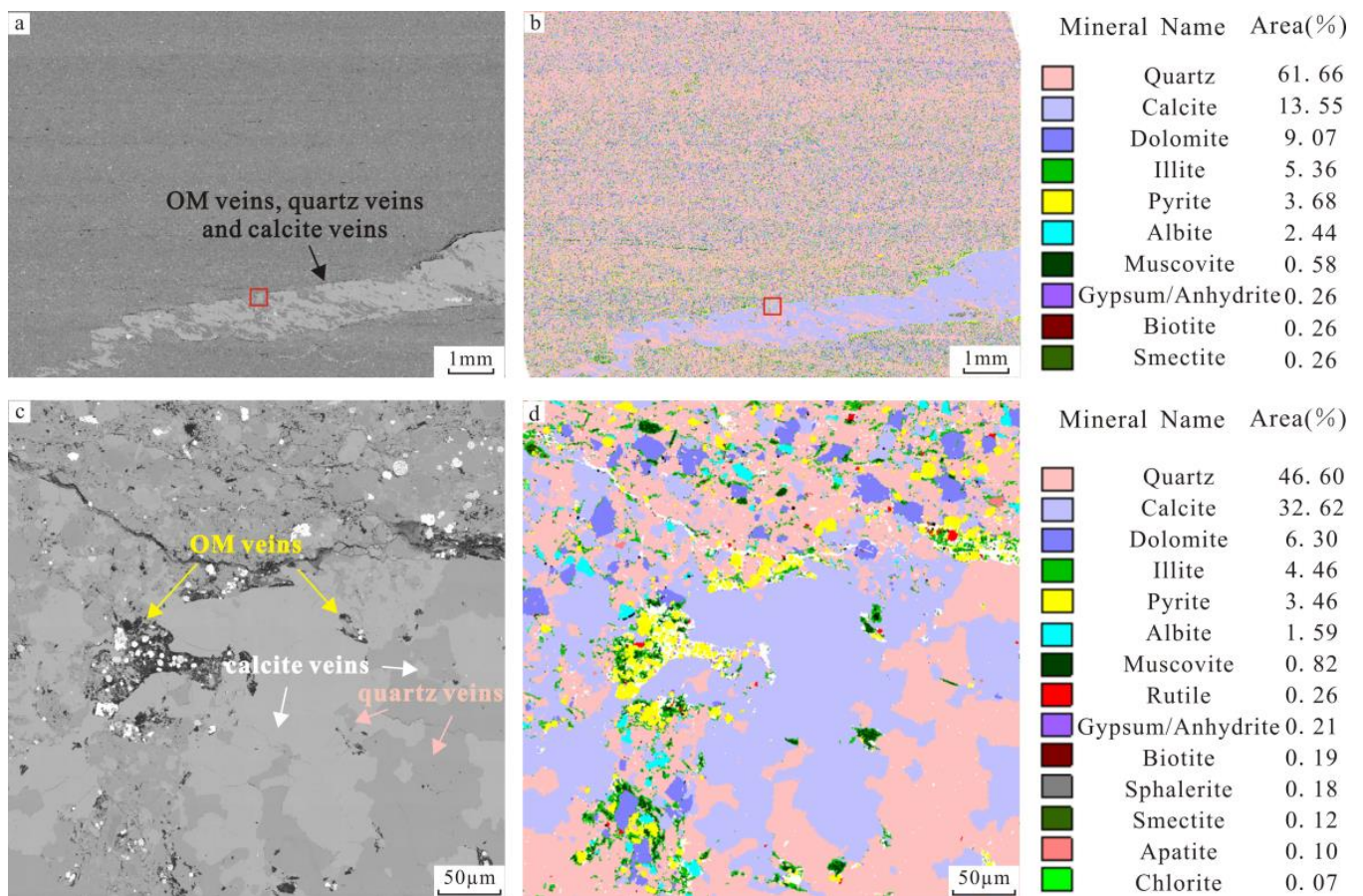


**Figure 3.** Scanning electron microscope image of Lu203H57-3 well (Long<sub>1</sub><sup>1</sup> layer, 3742.9 m). (a) MAPS scan image (500 nm resolution), visible veins. (b) QEMSCAN scanning image (15 μm resolution). (c) Figure 3a amplified image, MAPS scan image (4 nm resolution), the characteristics of organic matter vein, quartz vein and calcite vein can be seen. (d) Figure 3b amplified image, QEMSCAN scanning image (1 μm resolution).

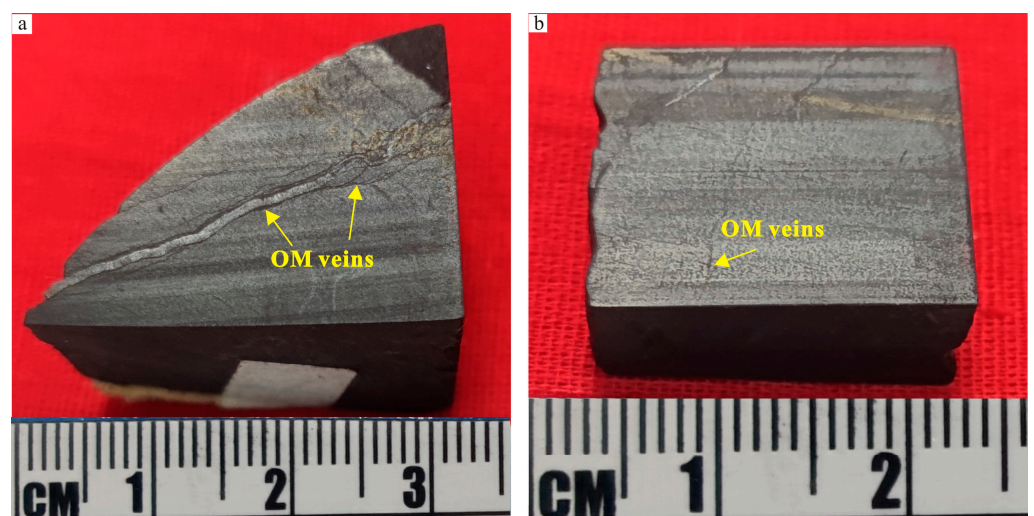


**Figure 4.** Core photos of Long<sub>1</sub> sub-member of Lu203H57-3 well. (a) Long<sub>1</sub><sup>2</sup> layer, 3740.6 m, OM veins can be seen under the light source. (b) Long<sub>1</sub><sup>1</sup> layer, 3743.8 m, OM veins can be seen under the light source.

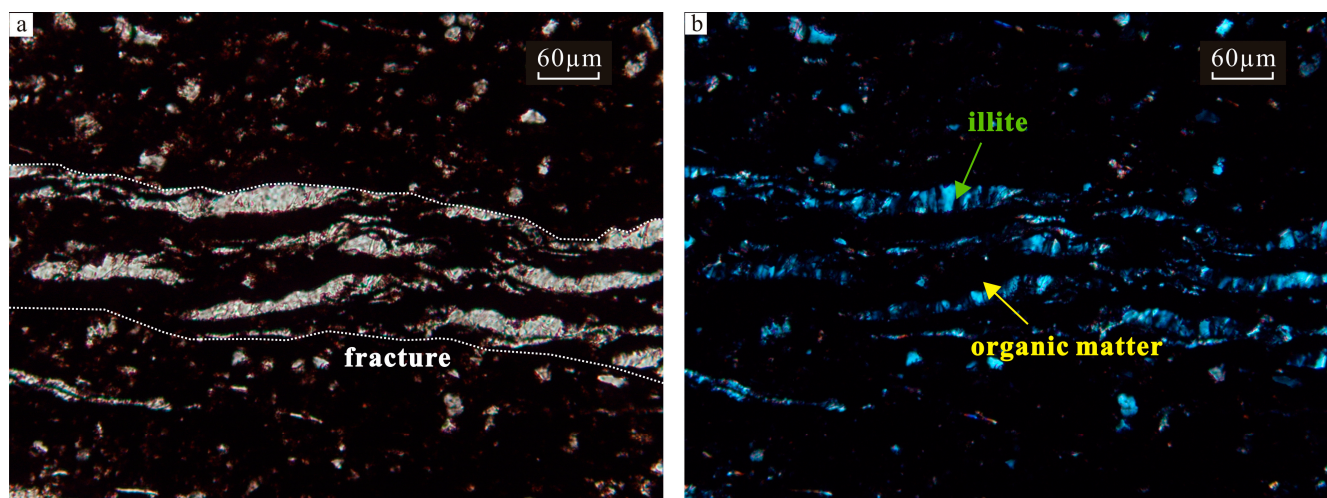


**Figure 5.** The thin section of Long<sub>1</sub><sup>2</sup> sub-member of Lu203H57-3 well. (a) Long<sub>1</sub><sup>2</sup> layer, 3741.8 m, filled with organic matter and illite in horizontal fractures (plane polarized light). (b) Long<sub>1</sub><sup>2</sup> layer, 3741.8 m, filled with organic matter and illite in horizontal fractures (perpendicular polarized light).

At the same time, quartz and calcite mineral veins can be seen around some organic veins (Figure 3). According to the occurrence state between the veins, the OM veins mostly appear on the fracture wall, and some appear inside the quartz and calcite veins (Figure 3c,d). Quartz is mostly isolated growth, discrete distribution, local across the crack wall, visible “quartz bridge” phenomenon [38]. The calcite veins are filled in the main space of the fracture, and the quartz veins are mostly wrapped (Figure 3).

#### 4.2. Reservoir Characteristics

Firstly, the pore-forming ability of different organic matter types was analyzed. The pore size distribution of in situ organic matter pores is wide, mostly in 20~200 nm, and the pore formation efficiency is high, with an average of 28.5% (Figure 2a,b, Table 1). As a contrast, the pores of organic matter migrating to inorganic pores are small and dense, mostly in the range of 20~100 nm, and the average pore formation efficiency is 10.7% (Figure 2c,d, Table 1). OM veins have the worst pore-forming ability, their average pore-forming efficiency is 2.4%. The pores are sparse, and the size of them is mostly 20~70 nm (Figures 6 and 7, Table 1).

**Table 1.** Comparison of pore-forming efficiency of different organic matter based on MAPS two-dimensional image.

Organic Matter Type	Pore-Forming Efficiency	Pore Characteristics
In situ organic matter	0%~60% (avg. 28.5%)	The pores are alternate in size and dense, mostly 20~300 nm
Organic matter in inorganic pores	3%~22% (avg. 10.7%)	The pores are small and dense, mostly 20~100 nm
Organic matter veins	0.3%~2.9% (avg. 2.4%)	The pores are sparse, mostly 20~70 nm

This study also further identifies the quality of the reservoir in the organic veins. Data display that the brittle mineral content of the samples with OM veins is more than 70%, with an average of 78.98%, while the brittle mineral content of the samples without OM veins is lower, ranging from 50% to 75%, with an average of 61.09%. The average organic porosity of the samples with OM veins is 2.18%, while the average organic porosity of the samples without OM veins is 1.72%. The samples with OM veins have higher brittle mineral content and organic porosity and are mostly developed in Long<sub>1</sub><sup>1</sup> and Long<sub>1</sub><sup>2</sup>

layers. For TOC content, the average TOC of samples with organic matter veins is 3.69%, while the average TOC of samples without organic matter veins is 3.4%. The TOC content of samples with OM veins development is slightly higher, and the overall difference is not significant (Table 2).

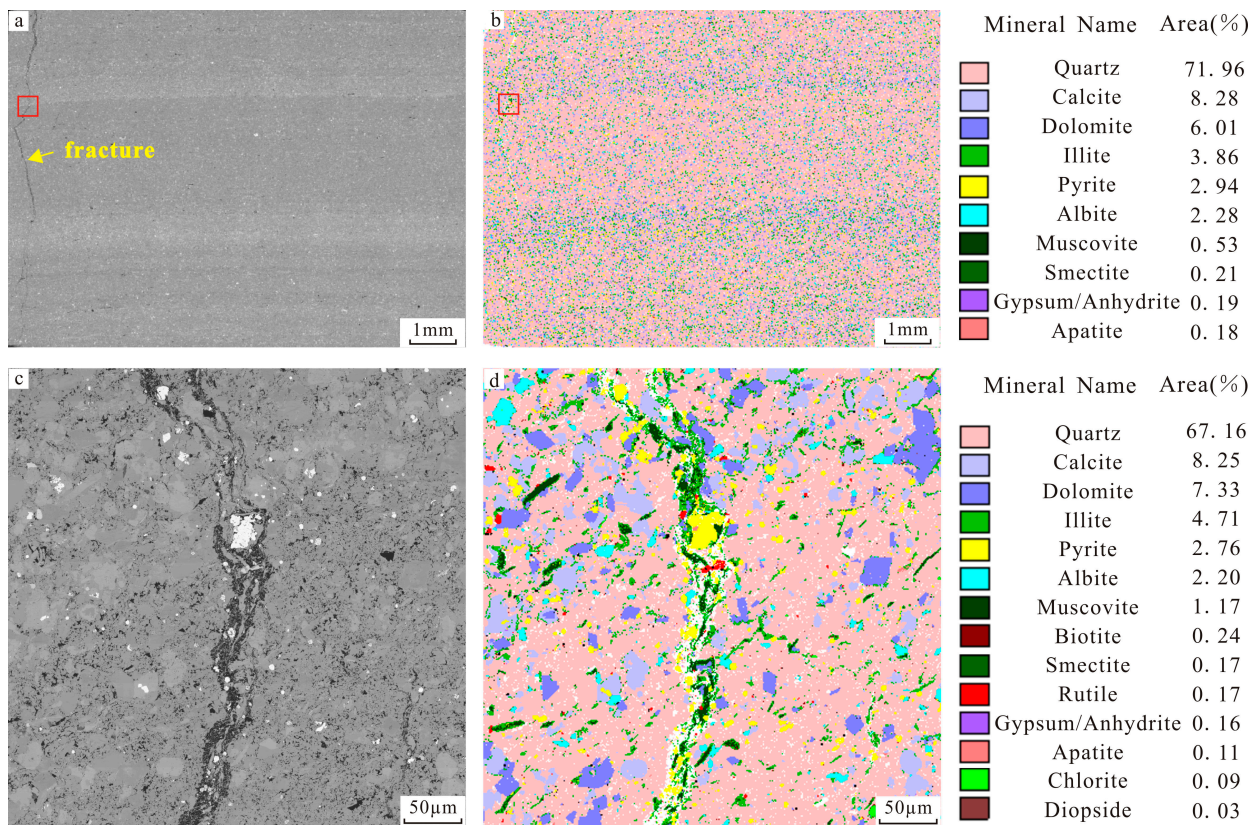


**Figure 6.** Scanning electron microscope image of Lu203H57-3 well (Long<sub>1</sub><sup>1</sup> layer, 3743.8 m). (a) MAPS scan image (500 nm resolution), visible fractures. (b) QEMSCAN scanning image (15 μm resolution). (c) Figure 6a amplified image in red squares, MAPS scan image (4 nm resolution), visible organic matter vein characteristics. (d) Figure 6b amplified image in red squares, QEMSCAN scanning image (1 μm resolution), visible mineral composition around the OM veins.

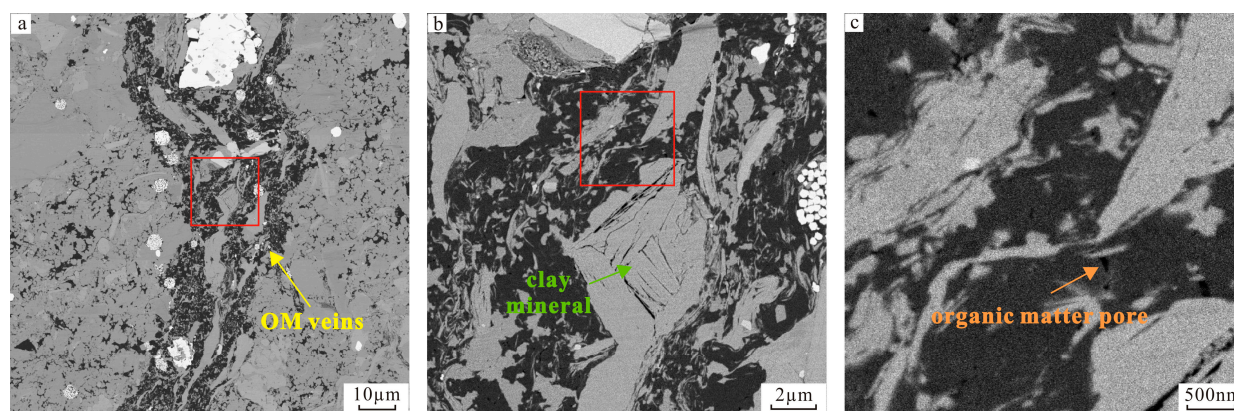


**Figure 7.** MAPS scanning electron microscopy (4 nm resolution) of Lu203H57-3 well (Long<sub>1</sub><sup>1</sup> layer, 3743.8 m). (a) OM veins. (b) Figure 7a amplified image in red squares. (c) Figure 7b amplified image in red squares, visible organic pores.

**Table 2.** Shale reservoir parameters of Long<sub>1</sub> sub-member in Lu203H57-3 well.

Depth/m	Layer	Quartz Content/%	Calcite Content/%	Brittle Minerals (Quartz + Calcite) Content/%	Organic Porosity/%	Vein Development	Vein Types	TOC
3730.7	Long <sub>1</sub> <sup>4</sup>	48.04	6.87	54.91	1.0	-	-	2.57
3733.2	Long <sub>1</sub> <sup>3</sup>	64.28	0.93	71.85	1.8	-	-	2.82
3734.9	Long <sub>1</sub> <sup>3</sup>	64.70	3.33	65.63	1.5	-	-	3.71
3735.6	Long <sub>1</sub> <sup>3</sup>	49.99	0.92	50.91	1.8	+	Quartz veins and calcite veins	3.81
3737.6	Long <sub>1</sub> <sup>2</sup>	58.85	3.28	62.13	2.5	-	-	4.10
3740.6	Long <sub>1</sub> <sup>2</sup>	59.58	10.71	70.29	1.8	++	OM veins, quartz veins and calcite veins	3.42
3741.8	Long <sub>1</sub> <sup>2</sup>	76.44	4.46	80.90	1.9	+	OM veins	3.15
3742.9	Long <sub>1</sub> <sup>1</sup>	69.66	13.55	83.21	2.7	++	OM veins, quartz veins and calcite veins	3.52
3743.8	Long <sub>1</sub> <sup>1</sup>	73.52	7.99	81.51	2.3	+	OM veins	4.68

Note: - means not seen; + means rare; ++ means common.

## 5. Discussion

### 5.1. Formation Mechanism of OM Veins

The occurrence of fractures filled with OM veins varies greatly, including horizontal, oblique and high-angle fractures, the opening is mostly 5–80 μm. According to the above occurrence and the characteristics of filling materials, the formation of this fracture is related to abnormal fluid high pressure [39,40].

Microscopic observation shows that the organic matter filled in the fracture is associated with clay minerals. Previous studies have shown that the mixture of the original deposited structural organic matter and clay minerals is quite common in Marine shales, this is due to the crystal structure and huge specific surface area of clay minerals, which have a strong ability to adsorb organic matter [41]. The mixture of the organic matter and clay minerals in the study section usually occurs in the following two forms. One is acicular clay minerals interwoven in organic matter (Figure 8a,c), and the other is organic matter in clay minerals (Figure 8b,d); organic pores are developed in both of them, which have the potential for hydrocarbon generation. However, the occurrence of clay minerals near OM veins is different from the above; the contact interface between organic matter and clay minerals is sharply defined (Figure 7), there is no obvious tendency for them to contact, react and promote each other, and the lack of pore development of OM veins also indicates that clay minerals here do not promote the hydrocarbon generation process of OM veins. Therefore, we infer that the charging period of OM veins is later based on their morphology and low porosity efficiency.

Therefore, according to the above microscopic characteristics, the formation and evolution process of OM veins is restored. With the continuous burial depth and temperature increase, the maturity of organic matter in the study section gradually increased ( $R_o > 0.5\%$ ) and entered the oil window; kerogen-generated liquid hydrocarbons with low density [42] were transported and filled into inorganic pores in a dispersed form [43]. With the increase in temperature, hydrocarbon generation of organic matter, dehydration of clay minerals, etc., the pore fluid pressure rises [44], and the pore fluid pressure cannot be released, exceeding the shale fracture limit and producing microfractures. The local expansion of micro-fractures forms an effective reservoir space, which releases stress. At the same time, driven by the pressure difference (negative pressure), the soluble organic matter fluid in the source rock of the study section fills into the fractures along the effective channels (pore throats, micro-fractures, kerogen networks, etc.) to form OM veins [45].

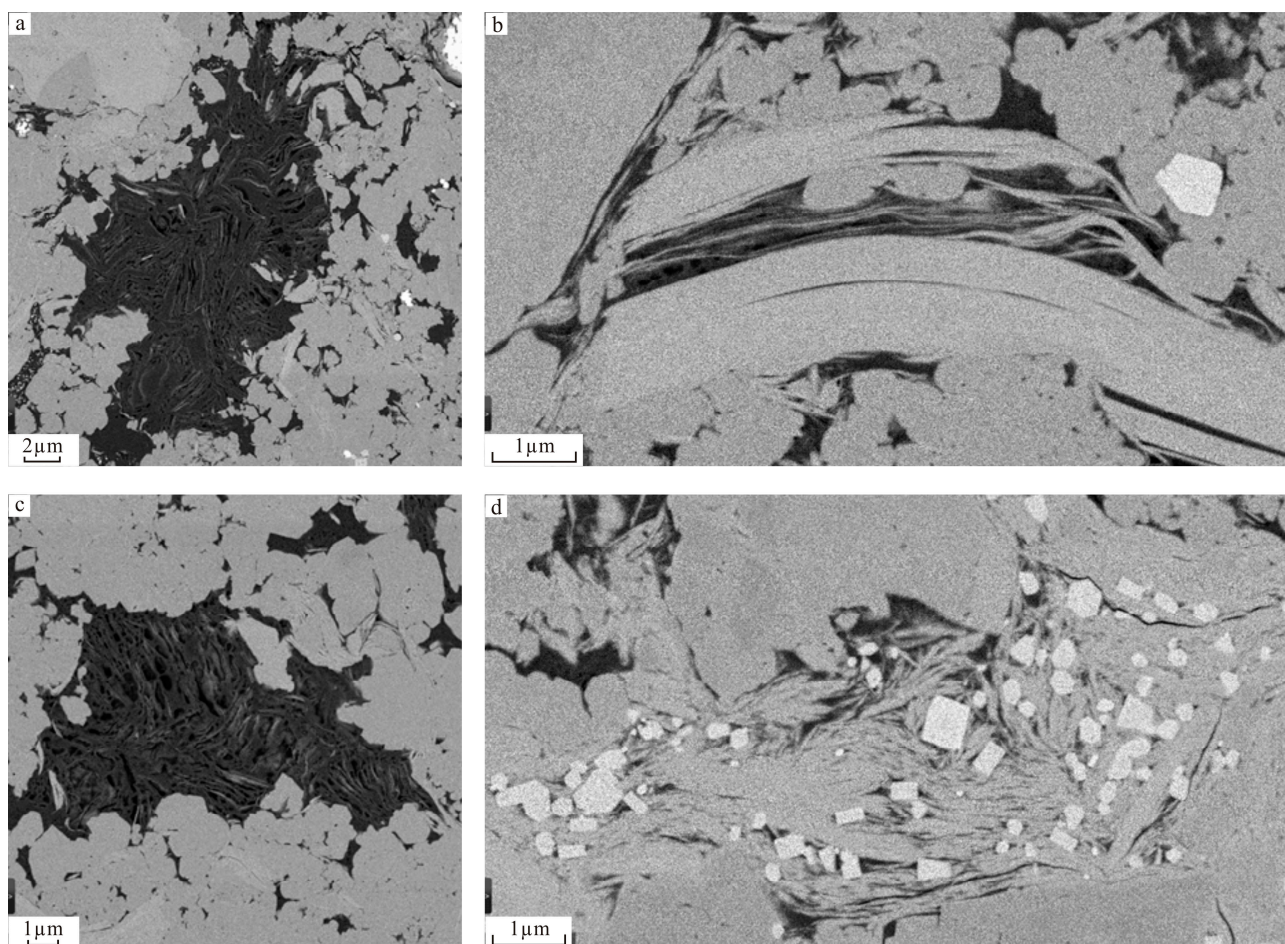


**Figure 8.** MAPS scanning electron microscopy (4 nm resolution) of the organic matter and clay minerals mixture. (a) Acicular clay minerals are interwoven in organic matter, in which a large number of organic pores are developed (Long<sub>1</sub><sup>1</sup> layer, 3743.8 m). (b) Organic matter in clay minerals developed well-rounded organic pores (Long<sub>1</sub><sup>2</sup> layer, 3737.6 m). (c) Acicular clay minerals are interwoven in organic matter, in which a large number of organic pores are developed (Long<sub>1</sub><sup>2</sup> layer, 3737.6 m). (d) Idiomorphic pyrite supports the interlayer fractures of clay minerals, which are filled with organic matter (Long<sub>1</sub><sup>3</sup> layer, 3733.2 m).

### 5.2. Formation Period of OM Veins

The OM veins and organic matter in inorganic pores are both from the more active organic matter in the in situ organic matter, which migrates in the form of liquid hydrocarbon after the oil generation window and should have good hydrocarbon-generation potential. However, the organic pores in OM veins are poorly developed, even in the presence of a large number of clay minerals as hydrocarbon-generating catalysts (Figure 7). At the same time, the pore-forming efficiency of OM veins is lower than that of in situ organic matter and organic matter in inorganic pores (Table 1), which indicates that organic matter vein formed in a later period, so it experienced a shorter hydrocarbon generation time and a lower degree of pore development. This also makes sense in principle, when organic matter continues to generate hydrocarbons, the intergranular pores are gradually occupied by migrating organic matter, the effect of increasing hydrocarbon-generation pressure will become more and more obvious, and eventually lead to shale reaching the rupture limit and generating abnormally high-pressure-related fractures, then organic matter veins can be formed.

According to the occurrence state of shale fracture composite veins in the study section, organic matter appears inside quartz and calcite veins (Figure 3). Quartz is mostly

isolated growth, discrete distribution, local across the crack wall, visible “quartz bridge” phenomenon [38]; the calcite veins are filled in the main space of the fracture, and the quartz veins are mostly wrapped (Figure 9). Based on the above contact relationship, OM veins are formed first, then quartz veins, and then calcite veins. At the same time, according to the previous test methods such as cathodoluminescence and inclusions to restore paleotemperature and pressure of the mineral veins in the study interval, it is shown that the quartz and calcite veins were formed after the kerogen in the interval became gas [46,47], which further indicates that the OM veins were formed before the filling of the mineral veins.

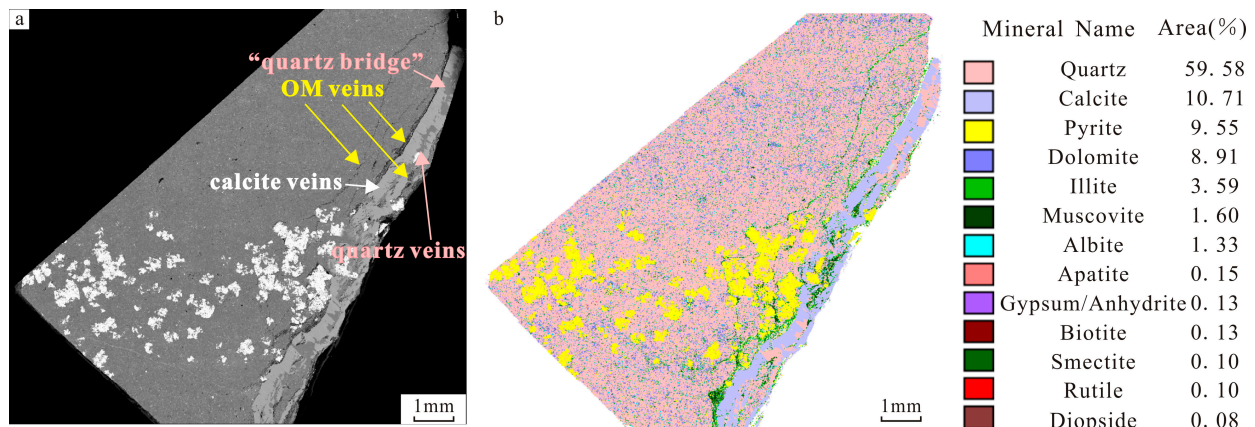


**Figure 9.** Scanning electron microscope image of Lu203H57-3 well (Long<sub>1</sub><sup>2</sup> layer, 3740.6 m). (a) MAPS scan image (500 nm resolution), OM veins, quartz veins and calcite veins can be seen. (b) QEMSCAN scanning image (15 μm resolution).

In summary, the OM veins were formed after shale reached the fracture limit, in the late stage of organic matter migration to inorganic pores, and before gas generation and mineral veins are filled.

### 5.3. Geological Significance of OM Veins

According to the formation mechanism of OM veins, the formation of OM veins requires the existence of overpressure gas reservoirs in the source rocks at that time to reach the fracture limit of shale [48]. Under the same tectonic stress, the higher the brittleness of shale, the smaller the strain before fracture. Therefore, the development degree of fractures in shale is usually positively correlated with the content of quartz and calcite, and negatively correlated with clay minerals [49,50]. The data show that the content of brittle minerals is higher in the interval of OM veins developed in Long<sub>1</sub> sub-member of the Luzhou area (Figure 10a), which indicates that the high-pressure-related fractures provided storage space for the occurrence of OM veins.

Simultaneously, the overpressure of the study section is mainly caused by the expansion of fluid volume [44], in which the hydrocarbon generation pressurization of organic matter is the most important influencing factor [40]. In order to compare the difference of hydrocarbon generation intensity between the interval of developed and undeveloped OM veins, TOC and organic porosity of samples were, respectively, used for analysis in this manuscript. The TOC of the samples with OM veins was higher, but the difference was not significant, the obvious difference is that the organic porosity of them is higher (Figure 10b,c), which means the porosity of organic pores is obviously higher in the interval with OM veins. Previous studies have shown that organic matter can break through the large-scale development of organic pores on the surface of organic matter only when the expansion force of gas generation is strong enough [51], so high hydrocarbon generation intensity will lead to high porosity of organic pores. Therefore, the OM veins are mainly due to the high hydrocarbon generation intensity, which makes the organic matter continue to migrate to the fracture after filling the inorganic pores. And the low pore-forming

efficiency of OM veins mentioned earlier also suggests that it was formed later than that of most organic matter migrating to inorganic pores.

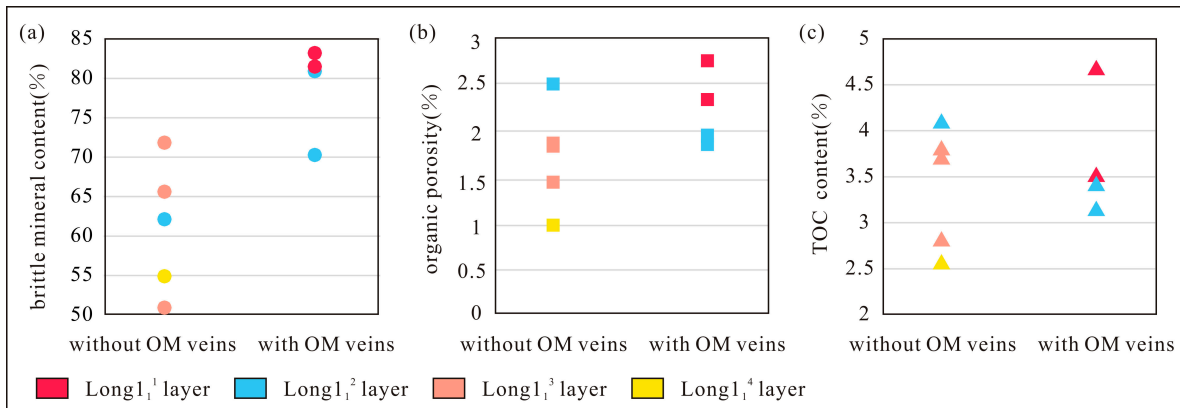


**Figure 10.** Correlation diagram of OM veins and reservoir parameters. (a) Correlation diagram of OM veins and brittle mineral content. (b) Correlation diagram of OM veins and organic porosity. (c) Correlation diagram of OM veins and TOC.

The OM veins are mostly developed in the Long<sub>1</sub><sup>1</sup> and Long<sub>1</sub><sup>2</sup> layers. The content of brittle minerals in this layer is high, which is conducive to the formation of cracks in the layer before gas generation, so that the basic space conditions for filling the OM veins are available. The high porosity of the organic pores in this section indicates that the organic matter has high hydrocarbon generation intensity and high hydrocarbon generation potential, so the soluble organic matter fills the inorganic pores and continues to migrate to the fractures to form OM veins (Figure 11). Therefore, the quality of Long<sub>1</sub><sup>1</sup> and Long<sub>1</sub><sup>2</sup> shale reservoirs with OM veins is better.

At the same time, combined with the source of OM veins and the factors affecting the formation of OM veins, it can be seen that the conditions that are not conducive to the development of OM veins in each layer of Long<sub>1</sub><sup>1</sup> sub-member: some layers have no cracks before gas generation, and soluble organic matter cannot be filled; there are cracks in the interval before gas generation, but the organic matter content is low or the hydrocarbon generation intensity is weak, and the organic matter is not filled into the cracks.

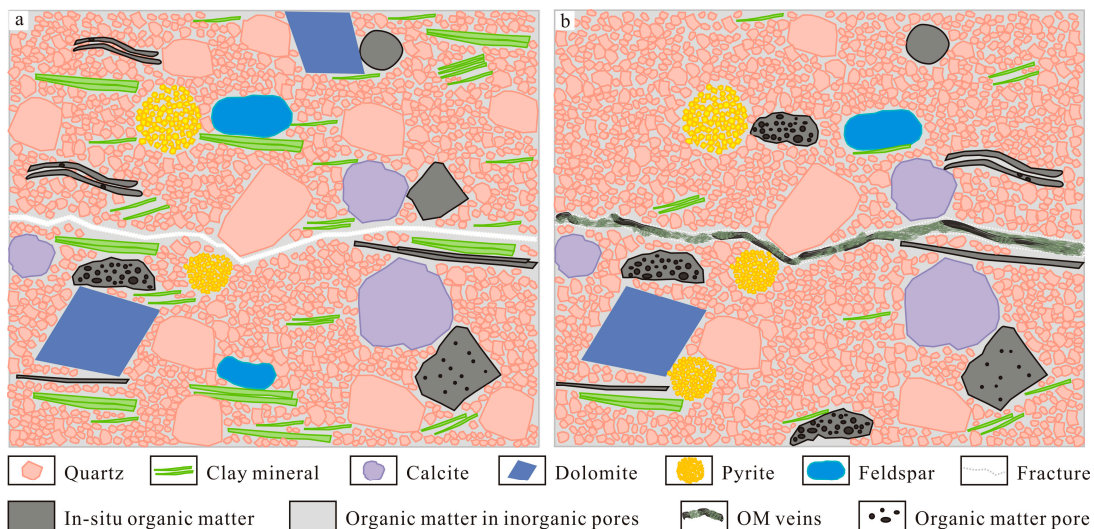


**Figure 11.** Pattern diagram of OM veins. (a) The section without OM veins has higher clay mineral content. (b) In the section with OM veins, the content of brittle minerals is higher, and the hydrocarbon generation potential of organic matter is higher.

In summary, the high hydrocarbon generation intensity and high brittle mineral content of shale reservoirs make the formation of OM veins, and the closed diagenesis system also provides good reservoir space for deep shale gas reservoirs [52]. Therefore, the existence of OM veins can indicate better reservoir conditions. The representative horizon has strong hydrocarbon generation intensity and high brittle mineral content, indicating that the horizon has shale gas enrichment conditions and good compressibility. It is a good geological–engineering dessert.

## 6. Conclusions

- (1) The OM veins mainly appear on the fracture wall, and some appear inside the quartz and calcite veins, most of them developed in the Long<sub>1</sub><sup>1</sup> and Long<sub>1</sub><sup>2</sup> layers.
- (2) The pore-forming efficiency of OM veins is lower than that of in-situ organic matter and organic matter in inorganic pores, the pores in the OM veins are sparse and the pore size is small.
- (3) The OM veins were formed after shale reached the fracture limit, in the late stage of organic matter migration to inorganic pores, and before mineral veins are filled.
- (4) The existence of OM veins can indicate high-quality reservoir conditions. The representative horizons have strong hydrocarbon generation strength (strong pore-forming ability of organic matter) and high brittle mineral content (strong reservoir compressibility), which makes the horizons conducive to shale gas accumulation and fracturing.

**Author Contributions:** Conceptualization, Y.W. and Y.J.; methodology, D.H.; software, C.W.; validation, W.L., D.H. and J.Z.; formal analysis, Y.J.; investigation, Y.W.; resources, W.L.; data curation, C.W.; writing—original draft preparation, Y.J.; writing—review and editing, Y.W.; visualization, B.M.; supervision, H.W.; project administration, C.W.; funding acquisition, D.H. All authors have read and agreed to the published version of the manuscript.

**Funding:** This work is funded by the National Natural Science Foundation of China (42072121) and the Natural Science Foundation of Hubei Province (2021CFB182).

**Data Availability Statement:** The data that support the findings of this study are available from the corresponding author upon reasonable request.

**Conflicts of Interest:** The authors declare that they have no conflict of interest.

## References

1. Qiu, Z.; Zou, C.N. Controlling factors on the formation and distribution of “sweet-spot areas” of marine gas shales in South China and a preliminary discussion on unconventional petroleum sedimentology. *J. Asian Earth Sci.* **2020**, *194*, 103989.
2. Jarvie, D.M.; Hill, R.J.; Ruble, T.E.; Pollastro, R.M. Unconventional shale-gas systems: The Mississippian Barnett Shale of north-central Texas as one model for thermogenic shale-gas assessment. *AAPG Bull.* **2007**, *91*, 475–499.
3. Wang, P.W.; Nie, H.K.; Liu, Z.B.; Sun, C.X.; Cao, Z.; Wang, R.Y.; Li, P. Differences in Pore Type and Pore Structure between Silurian Longmaxi Marine Shale and Jurassic Dongyuemiao Lacustrine Shale and Their Influence on Shale-Gas Enrichment. *Minerals* **2023**, *13*, 190.
4. Loucks, R.G.; Reed, R.M.; Ruppel, S.C.; Hammes, U. Spectrum of pore types and networks in mudrocks and a descriptive classification for matrix-related mudrock pores. *AAPG Bulletin.* **2012**, *96*, 1071–1098. [[CrossRef](#)]
5. Jia, Y.Q.; Han, D.L.; Zhang, J.Z.; Wang, C.C.; Lin, W.; Ren, X.H.; Yang, C.Y.; Chang, L.C. Differences in Pore forming Efficiency among Organic Macerals and Its Restriction against Reservoir Quality: A Case Study Based on the Marine Shale Reservoir in the Longmaxi Formation, Southern Sichuan Basin, China. *Lithosphere* **2021**, *97*, 2700912.
6. Wang, R.Y.; Hu, Z.Q.; Long, S.X.; Du, W.; Wu, J.; Wu, Z.H.; Nie, H.K.; Wang, P.W.; Sun, C.X.; Zhao, J.H. Reservoir characteristics and evolution mechanisms of the Upper Ordovician Wufeng-Lower Silurian Longmaxi shale, Sichuan Basin. *Oil Gas Geol.* **2022**, *43*, 353–364.
7. Jia, Y.Q.; Liu, Z.P.; Ren, X.H.; Zhou, Y.B.; Zheng, A.L.; Zhang, J.; Han, D.L. Organic matter type differentiation process and main control mechanism: Case study of the Silurian Longmaxi Formation shale reservoir in Weiyuan area. *Acta Sedimentol. Sin.* **2021**, *39*, 341–352.
8. Hu, Z.Q.; Du, W.; Peng, Y.M.; Zhao, J.H. Microscopic pore characteristics and the source-reservoir relationship of shale—A case study from the Wufeng and Longmaxi Formations in Southeast Sichuan Basin. *Oil Gas Geol.* **2015**, *36*, 1001–1008.

9. Loucks, R.G.; Reed, R.M. Scanning-electron-microscope petrographic evidence for distinguishing organic-matter pores associated with depositional organic matter versus migrated organic matter in mudrocks. *Gcags Trans.* **2014**, *64*, 51–60.
10. Xie, G.L.; Liu, S.G.; Jiao, K.; Deng, B.; Ye, Y.H.; Sun, W.; Li, Z.Q.; Liu, W.P.; Luo, C.; Li, Z.C. Organic pores in deep shale controlled by macerals: Classification and pore characteristics of organic matter components in Wufeng Formation-Longmaxi Formation of the Sichuan Basin. *Nat. Gas Ind.* **2021**, *41*, 23–34.
11. Cardott, B.J.; Landis, C.R.; Curtis, M.E. Post-oil solid bitumen network in the Woodford Shale, USA-A potential primary migration pathway. *Int. J. Geol.* **2015**, *139*, 106–113.
12. Wang, P.F.; Jiang, Z.X.; Lyu, P.; Jin, C.; Li, X.; Huang, P. Organic matter pores and evolution characteristics of shales in the Lower Silurian Longmaxi Formation and Lower Cambrian Niutitang Formation in periphery of Chongqing. *Nat. Gas Geosci.* **2018**, *29*, 997–1008.
13. Curtis, M.E.; Cardott, B.J.; Sondergeld, C.H.; Rai, C.S. Development of organic porosity in the Woodford Shale with increasing thermal maturity. *Int. J. Coal Geol.* **2012**, *103*, 26–31.
14. Gao, Z.; Fan, Y.; Xuan, Q.; Zheng, G. A review of shale pore structure evolution characteristics with increasing thermal maturities. *Adv. Geo-Energy Res.* **2020**, *4*, 247–259.
15. Wang, R.Y.; Hu, Z.Q.; Nie, H.K.; Liu, Z.B.; Chen, Q.; Gao, B.; Liu, G.X.; Gong, D.J. Comparative analysis and discussion of shale reservoir characteristics in the Wufeng-Longmaxi and Niutitang formations: A case study of the well JY1 in SE Sichuan Basin and well TX1 in SE Guizhou area. *Pet. Geol. Exp.* **2018**, *40*, 639–649.
16. Han, J.; Chen, B.; Zhao, X.B.; Zheng, C.; Zhang, J.M. Development characteristics and influential factors of organic pores in the Permian shale in the Lower Yangtze Region. *Nat. Gas Ind.* **2017**, *37*, 17–26.
17. Nie, H.K.; He, Z.L.; Wang, R.Y.; Zhang, G.R.; Chen, Q.; Li, D.H.; Lu, Z.Y.; Sun, C.X. Temperature and origin of fluid inclusions in shale veins of Wufeng-Longmaxi Formations, Sichuan Basin, south China: Implications for shale gas preservation and enrichment. *J. Pet. Sci. Eng.* **2020**, *193*, 107329.
18. Ougier-Simonin, A.; Renard, F.; Boehm, C.; Vidal-Gilbert, S. Microfracturing and microporosity in shales. *Earth-Sci. Rev.* **2016**, *162*, 198–226.
19. Tan, R.; Wang, R.Y.; Huang, Y.H.; Yang, R.; Li, H.B.; Lu, K. Mechanism of the Enrichment and Loss Progress of Deep Shale Gas: Evidence from Fracture Veins of the Wufeng-Longmaxi Formations in the Southern Sichuan Basin. *Minerals* **2022**, *12*, 897.
20. Yang, H.Z.; Zhao, S.X.; Liu, Y.; Wu, W.; Xia, Z.Q.; Wu, T.P.; Luo, C.; Fan, T.Y.; Yu, L.Y. Main controlling factors of enrichment and high-yield of deep shale gas in the Luzhou Block, southern Sichuan Basin. *Nat. Gas Ind.* **2019**, *39*, 55–63.
21. Dong, M.; Gou, W.; Zhang, L.Y.; Wu, Z.H.; Ma, L.C.; Dong, H.; Feng, X.Q.; Yang, Y.H. Characteristics of paleotectonic stress field and fractures of Wufeng-Longmaxi Formation in Luzhou area, southern Sichuan Basin. *Lithol. Reserv.* **2022**, *34*, 43–51.
22. Liu, Z.B.; Gao, B.; Zhang, Y.Y.; Du, W.; Feng, D.J.; Nie, H.K. Types and distribution of the shale sedimentary facies of the Lower Cambrian in Upper Yangtze area, South China. *Pet. Explor. Dev.* **2017**, *44*, 21–31.
23. Gou, T.L.; Zhang, H.R. Formation and enrichment mode of Jiaoshiha shale gas field, Sichuan Basin. *Pet. Explor. Dev.* **2014**, *41*, 28–36.
24. Guo, Y.H.; Li, Z.F.; Li, D.H.; Zhang, T.M.; Wang, Z.C.; Yu, J.F.; Xi, Y.T. Lithofacies palaeogeography of the Early Silurian in Sichuan area. *J. Palaeogeogr.* **2004**, *6*, 20–29.
25. Wang, X.M.; Liu, L.F.; Wang, Y.; Sheng, Y.; Zheng, S.S.; Luo, Z.H. Control of lithofacies on pore space of shale from Longmaxi Formation, southern Sichuan Basin. *Acta Pet. Sin.* **2019**, *40*, 1192–1201.
26. Ge, X.Y.; Mou, C.L.; Yu, Q.; Liu, W.; Men, X.; He, J.L. The geochemistry of the sedimentary rocks from the Huadi No. 1 well in the Wufeng-Longmaxi formations (Upper Ordovician-Lower Silurian), South China, with implications for paleoweathering, provenance, tectonic setting and paleoclimate. *Mar. Pet. Geol.* **2019**, *103*, 646–660.
27. Yan, C.N.; Jin, Z.J.; Zhao, J.H.; Du, W.; Liu, Q.Y. Influence of sedimentary environment on organic matter enrichment in shale: A case study of the Wufeng and Longmaxi Formations of the Sichuan Basin, China. *Mar. Pet. Geol.* **2018**, *92*, 880–894.
28. Wu, L.Y.; Lu, Y.C.; Jiang, S.; Liu, X.F.; He, G.S. Effects of volcanic activities in Ordovician Wufeng-Silurian Longmaxi period on organic-rich shale in the Upper Yangtze area, South China. *Pet. Explor. Dev.* **2018**, *45*, 806–816.
29. Pu, B.L.; Dong, D.Z.; Wang, F.Q.; Wang, Y.M.; Huang, J.L. The effect of sedimentary facies on Longmaxi shale gas in southern Sichuan Basin. *Geol. China* **2020**, *47*, 111–120.
30. Wang, S.F.; Dong, D.Z.; Wang, Y.M.; Li, X.J.; Huang, J.L.; Guan, Q.Z. Sedimentary geochemical proxies for paleoenvironment interpretation of organic-rich shale: A case study of the Lower Silurian Longmaxi Formation, southern Sichuan Basin, China. *J. Nat. Gas Sci. Eng.* **2016**, *28*, 691–699.
31. Zhao, S.X.; Yang, Y.M.; Zhang, J.; Wang, L.S.; Wang, X.Z.; Luo, C.; Tian, C. Micro-layers division and fine reservoirs contrast of Lower Silurian Longmaxi Formation shale, Sichuan Basin, SW China. *Nat. Gas Geosci.* **2016**, *27*, 470–487.
32. Gao, Z.Y.; Fan, Y.P.; Hu, Q.H.; Jiang, Z.X.; Huang, Z.L.; Wang, Q.Y.; Cheng, Y. Differential development characteristics of organic matter pores and their impact on reservoir space of Longmaxi Formation shale from the south Sichuan Basin. *Pet. Sci. Bull.* **2020**, *5*, 1–16.
33. Wu, J.G.; Yuan, Y.; Niu, S.Y.; Wei, X.F.; Yang, J.J. Multiscale characterization of pore structure and connectivity of Wufeng-Longmaxi shale in Sichuan Basin, China. *Mar. Pet. Geol.* **2020**, *120*, 104514.
34. Wang, H.; Zhou, S.; Li, S.; Zhao, M.; Zhu, T. Comprehensive characterization and evaluation of deep shales from Wufeng-Longmaxi Formation by LF-NMR technology. *Unconv. Resour.* **2022**, *2*, 1–11.

35. Guo, X.S.; Li, Y.P.; Borjigen, T.; Wang, Q.; Yuan, T.; Shen, B.J.; Ma, Z.L.; Wei, F.B. Hydrocarbon generation and storage mechanisms of deep-water shelf shales of Ordovician Wufeng Formation-Silurian Longmaxi Formation in Sichuan Basin, China. *Pet. Explor. Dev.* **2020**, *47*, 193–201.
36. Saif, T.; Lin, Q.Y.; Butcher, A.R.; Bijeljic, B.; Blunt, M.J. Multi-scale multi-dimensional microstructure imaging of oil shale pyrolysis using X-ray micro-tomography, automated ultra-high resolution SEM, MAPS Mineralogy and FIB-SEM. *Appl. Energy* **2017**, *202*, 628–647.
37. Schneider, C.A.; Rasband, W.S.; Eliceiri, K.W. NIH Image to ImageJ: 25 years of image analysis. *Nat. Methods* **2012**, *9*, 671–675.
38. Wang, Z.; Lyu, X.X.; Zhang, L.X.; Li, F.; Ouyang, S.Q.; Wang, R. Discovery of “quartz bridge” in Kuqa foreland thrust belt and its geological significance. *Earth Sci.* **2023**, *48*, 342–358.
39. Wang, X.X.; Wan, Y.L. Significance of the organic clay polymer on oil and gas generation. *China Offshore Oil Gas* **1993**, *7*, 27–33.
40. Zeng, L.B.; Ma, S.J.; Tian, H.; Xue, M.; Liu, G.P.; Lyu, W.Y. Research progress of natural fractures in organic rich shale. *Earth Sci.* **2022**, *48*, 1–15.
41. Zeng, L.B.; Qi, J.F.; Wang, Y.X. Origin type of tectonic fractures and geological conditions in low-permeability reservoirs. *Acta Pet. Sin.* **2007**, *28*, 52–56.
42. Lu, X.C.; Hu, W.X.; Fu, Q.; Miao, D.Y.; Zhou, G.J.; Hong, Z.H. Study of combination pattern of soluble organic matters and clay minerals in the immature source rocks in Dongying Depression, China. *Sci. Geol. Sin.* **1999**, *34*, 72–80.
43. Zhang, Q.; Liang, F.; Pang, Z.L.; Zhou, S.W.; Lin, W. Quantitative influence of soluble organic matter on pore structure in transitional shale. *Pet. Geol. Exp.* **2018**, *40*, 730–738.
44. Liu, D.D.; Guo, J.; Pan, Z.K.; Du, W.; Zhao, F.P.; Chen, Y.; Shi, F.L.; Song, Y.; Jiang, Z.X. Overpressure evolution process in shale gas reservoir: Evidence from the fluid inclusions in the fractures of Wufeng Formation-Longmaxi Formation in the southern Sichuan Basin. *Nat. Gas Ind.* **2021**, *41*, 12–22.
45. Zhi, F.Q.; Li, Q.; Fan, D.H.; Zhang, C.M. Study on migration and accumulation of fractured mudstone reservoirs in Zhanhua Sag. *Pet. Geol. Recovery Effic.* **2004**, *11*, 27–29.
46. Deng, M.; Duan, X.G.; Zhai, C.B.; Long, S.X.; Yang, Z.H.; Zheng, L.J.; Li, Z.C.; Cao, T.T. Variation in liquid hydrocarbon content during thermal simulation and its influence on physical property of shale. *Oil Gas Geol.* **2020**, *41*, 1310–1320.
47. Pan, Z.K.; Liu, D.D.; Huang, Z.X.; Jiang, Z.X.; Song, Y.; Guo, J.; Li, C.X. Paleotemperature and paleopressure of methane inclusions in fracture cements from the Wufeng-Longmaxi shales in the Luzhou area, southern Sichuan Basin. *Pet. Sci. Bull.* **2019**, *4*, 242–253.
48. Osborne, M.J.; Swarbrick, R.E. Mechanisms for generating overpressure in sedimentary basins: A reevaluation. *AAPG Bull.* **1997**, *81*, 1023–1041.
49. Tian, H.; Zeng, L.B.; Xu, X.; Shu, Z.G.; Peng, Y.M.; Mao, Z.; Luo, B. Characteristics of natural fractures in marine shale in Fuling area, Sichuan Basin, and their influence on shale gas. *Oil Gas Geol.* **2020**, *41*, 474–483.
50. Wu, Q.Y.; Han, D.L.; Zhang, J.Z.; Wang, C.C.; Ren, X.H.; Lin, Z.Z.; Su, M.M.; Zhu, Y.L.; Zhang, J. Influence of particle size effect on microfracture development in shale reservoir: A case study of the Silurian Longmaxi Formation shale reservoir in Weiyuan area. *J. Cent. South Univ. (Sci. Technol.)* **2022**, *53*, 3603–3614.
51. Ding, J.H.; Zhang, J.C.; Yang, C.; Huo, Z.P.; Lang, Y. Formation Evolution and Influencing Factors of Organic Pores in Shale. *J. Southwest Pet. Univ. (Sci. Technol. Ed.)* **2019**, *41*, 33–44.
52. Yao, C.P.; Fu, H.J.; Ma, Y.Z.; Yan, D.T.; Wang, H.; Li, Y.G.; Wang, J.W. Development characteristics of deep shale fractured veins and vein forming fluid activities in Luzhou block. *Earth Sci.* **2022**, *47*, 1684–1693.

**Disclaimer/Publisher’s Note:** The statements, opinions and data contained in all publications are solely those of the individual author(s) and contributor(s) and not of MDPI and/or the editor(s). MDPI and/or the editor(s) disclaim responsibility for any injury to people or property resulting from any ideas, methods, instructions or products referred to in the content.